Journal of Materials and Engineering Structures

Research Paper

Modelling of Creep Rupture in Clay using the Bounding Surface Viscoplasticity Theory

Thi Ngoc Mac [a,]*, Babak Shahbodagh [b], Nasser Khalili [b]

[a] *Thuyloi University, 175 Tay Son, Dong Da, Hanoi, Vietnam*

[b] *The University of New South Wales, UNSW Sydney, NSW 2052 Australia*

ARTICLE INFO

Article history:

Received : 23 November 2020

Revised : 28 December 2020

Accepted : 28 December 2020

Keywords:

Tertiary Creep

Clay

Bounding Surface

Viscoplasticity

ABSTRACT

The creep process is generally defined into three stages: primary, secondary and tertiary creep. Tertiary creep is the last phase among the three phases of creep process, where the strain rate accelerates until creep rupture occurs. This paper presents a viscoplastic constitutive model and demonstrates the capability of the model to capture tertiary creep and creep rupture. The model is based on the bounding surface plasticity and the viscoplastic consistency framework. It meets the consistency condition and allows a seamless transition from rate-independent plasticity to rate-dependent viscoplasticity. The rate-dependency is achieved through defining the bounding surface as a function of viscoplastic volumetric strain and viscoplastic volumetric strain rate. Simulation results and comparison with experimental data are presented for a set of undrained creep tests on normally consolidated soil and drained creep tests on heavily over-consolidated clay to show the application of the model in capturing the tertiary creep in clayey soils.

F. ASMA & H. HAMMOUM (Eds.) special issue, 3rd International Conference on Sustainability in Civil Engineering ICSCE 2020, Hanoi, Vietnam, J. Mater. Eng. Struct. 7(4) (2020)

1 Introduction

The time-dependent behaviour of cohesive soils, especially creep and creep rupture has been of great interest in geotechnical engineering practice. The overstress theory was widely used in elasto-viscoplastic models to describe the time-dependent behaviour of geomaterials. Most elasto-viscoplastic models are based on either the concept of overstress theory [1, 2] and the critical state framework [3-9], or the nonstationary flow surface theory [10-12]. However, there were very few overstress type models which can capture the drained tertiary creep process and creep failure in over-consolidated clays. It is special importance for stability analyses of slopes where creep ruptures are most common.

A viscoplastic constitutive model is presented in this paper to capture creep in clays including tertiary creep and creep rupture. The model is formulated based on the bounding surface plasticity model [13] and the viscoplastic consistency

* *Corresponding author. Tel.: +84365382317.*
E-mail address: ngocmt@tlu.edu.vn

RESEARCH REVIEW of Sciences and Technologies

e-ISSN: 2170-127X,

theory[14, 15]. The viscoplastic strain and strain rate effects on the soil strength are considered through controlling the size of the bounding surface. Unlike the overstress based constitutive models, the proposed viscoplastic model meets the consistency condition. Within this context, the model is able to capture drained and undrained creep rupture in clays.

2 Bounding Surface Viscoplasticity Model

The model is the extension of the bounding surface plasticity model [13] using the consistency theory [14, 15]. The essential elements of the model are: elastic properties, bounding and loading surfaces, viscoplasticity flow rule, and hardening rule. The total strain rate can be decomposed into elastic (e) and viscoplastic (vp) components as

$$\dot{\boldsymbol{\varepsilon}} = \dot{\boldsymbol{\varepsilon}}^{e} + \dot{\boldsymbol{\varepsilon}}^{vp} \tag{1}$$

where $\dot{\boldsymbol{\varepsilon}}^{e}$ and $\dot{\boldsymbol{\varepsilon}}^{vp}$ are the elastic and viscoplastic strain rates, respectively. The elastic response can be described using a stress-strain relationship as

$$\dot{\boldsymbol{\sigma}}' = \mathbf{D}^{e}\dot{\boldsymbol{\varepsilon}}^{e} \tag{2}$$

where $\dot{\boldsymbol{\sigma}}'$ is the stress rate and $\mathbf{D}^{e}$ is the elastic stiffness matrix.

2.1 Bounding and loading surfaces

The bounding surface adopted is described as [16]

$$F(\bar{p}', \bar{q}, \bar{p}'_{c}) = \left(\frac{\bar{q}}{M_{cs}\bar{p}'}\right)^{N} - \frac{\ln(\bar{p}'_{c}/\bar{p}')}{\ln R} = 0 \tag{3}$$

where $\bar{p}'_{c}$ controls the size of F and is a function of the viscoplastic volumetric strain ε_{p}^{vp} and strain rate $\dot{\varepsilon}_{p}^{vp}$, the material constant R represents the ratio between $\bar{p}'_{c}$ and the value of $\bar{p}'$ at the intercept of F with the CSL in the $(q\sim p')$ plane, the material constant N controls the curvature of the surface, and the superimposed bar denotes stress conditions on the bounding surface.

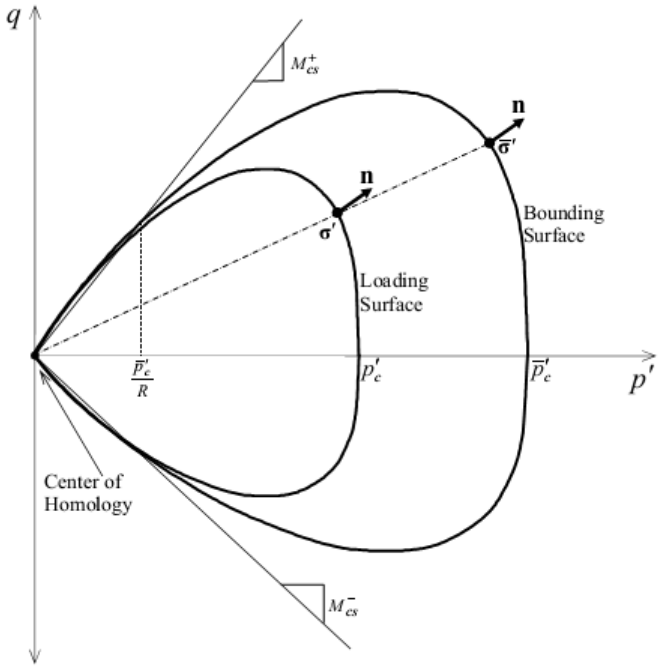

Fig. 1. Bounding surface, loading surface and image point in the $(q\sim p')$ plane

The loading surface adopted is of the same shape and is homologous to the bounding surface about the origin in the $(q\sim p^{'})$ plane. The function for the loading surface takes the form

$$f(p',q,p'_c) = \left(\frac{q}{M_{cs}p'}\right)^N - \frac{\ln(p'_c/p')}{\ln R} = 0 \tag{4}$$

where p'_c is the hardening parameter controlling the size of the loading surface. The image point is defined using a mapping rule such that a straight line passing through the centre of homology and $\boldsymbol{\sigma}'$ intersects the bounding surface at $\bar{\boldsymbol{\sigma}}'$ having the same unit normal vector as $\boldsymbol{\sigma}'$ on the loading surface (Figure. 1). The unit normal vector at the image point defining the direction of loading is given by

$$\mathbf{n} = \frac{\partial f/\partial \boldsymbol{\sigma}'}{\|\partial f/\partial \boldsymbol{\sigma}'\|} = \frac{\partial F/\partial \bar{\boldsymbol{\sigma}}'}{\|\partial F/\partial \bar{\boldsymbol{\sigma}}'\|} \tag{5}$$

2.2 Viscoplastic potential

The viscoplastic potential defines the direction of viscoplastic strain increments and is generally expressed using a plastic flow rule relating the plastic dilatancy to the stress ratio as

$$d = \frac{\dot{\boldsymbol{\varepsilon}}_p^{vp}}{\dot{\boldsymbol{\varepsilon}}_q^{vp}} = \bar{\tilde{t}} A \left(M_{cs} - \frac{q}{p'}\right) \tag{6}$$

where A is a material constant dependent on the mechanism and amount of energy dissipation.

The viscoplastic potential g is obtained by integrating Eq. (6) with respect to p' and q as

$$g(p',q,p_0) = \bar{\tilde{t}}\left[q + \frac{AM_{cs}p'}{A-1}\left(\left(\frac{p'}{p_0}\right)^{A-1} - 1\right)\right] \tag{7}$$

in which p_0 is the variable controlling the size of the viscoplastic potential.

The direction of viscoplastic flow is defined as

$$\mathbf{m} = \frac{\partial g/\partial \boldsymbol{\sigma}'}{\|\partial \mathrm{g}/\partial \boldsymbol{\sigma}'\|} \tag{8}$$

2.3 Hardening rule

The hardening rule defines the variation of the size and the location of the loading and bounding surfaces with respect to the variation of viscoplastic strain and the viscoplastic strain rate. In this model, the strain hardening modulus h can be divided into two components

$$h = h_b + h_f \tag{9}$$

where h_b is the viscoplastic strain hardening modulus at the image point $\bar{\boldsymbol{\sigma}}'$ on the bounding surface, and h_f is some arbitrary modulus at $\boldsymbol{\sigma}'$, defined as a function of the distance between $\bar{\boldsymbol{\sigma}}'$ and $\boldsymbol{\sigma}'$.

The strain hardening modulus h_f is defined such that it is zero on the bounding surface and infinity at the point of stress reversal as

$$h_f = \tilde{t}\frac{\partial \bar{p}'_c}{\partial \varepsilon_p^{vp}}\frac{p'}{\bar{p}'_c}\left[\frac{\bar{p}'_c}{\hat{p}'_c} - 1\right] k_m(\eta_p - \eta) \tag{10}$$

where $\eta_p = M_{cs}\left(1 - 2(\upsilon - \upsilon_{cs})\right)$ is the slope of the peak strength line in the $(q - p')$ plane and k_m is a material parameter controlling the steepness of the response in the $(q - \varepsilon_q)$ plane.

Applying the consistency condition to the bounding surface yields

$$\dot{F} = \left(\frac{\partial F}{\partial \bar{\boldsymbol{\sigma}}'}\right)^T \dot{\bar{\boldsymbol{\sigma}}}' + \frac{\partial F}{\partial \bar{p}'_c}\frac{\partial \bar{p}'_c}{\partial \varepsilon_p^{vp}}\dot{\varepsilon}_p^{vp} + \frac{\partial F}{\partial \bar{p}'_c}\frac{\partial \bar{p}'_c}{\partial \dot{\varepsilon}_p^{vp}}\ddot{\varepsilon}_p^{vp} = 0 \tag{11}$$

Eq. (11) can also be rewritten as

$$\mathbf{n}^T \dot{\bar{\boldsymbol{\sigma}}}' m_p - h_b \dot{\varepsilon}_p^{vp} - \xi_b \ddot{\varepsilon}_p^{vp} = 0 \tag{12}$$

where
$$h_b = -\frac{\partial F}{\partial \bar{p}'_c}\frac{\partial \bar{p}'_c}{\partial \varepsilon_p^{vp}}\frac{m_p}{\|\partial F/\partial \bar{\boldsymbol{\sigma}}'\|} \tag{13}$$

and ξ_b is the viscoplastic strain rate hardening modulus,

$$\xi_b = -\frac{\partial F}{\partial \bar{p}'_c}\frac{\partial \bar{p}'_c}{\partial \dot{\varepsilon}_p^{vp}}\frac{m_p}{\|\partial F/\partial \bar{\boldsymbol{\sigma}}'\|} \tag{14}$$

where
$$m_p = \partial g/\partial p'/\|\partial g/\partial \boldsymbol{\sigma}'\| \tag{15}$$

2.4 Elasto-Viscoplastic Stress-Strain Relationship

The constitutive relations for geomaterials are highly nonlinear, and hence, they are generally expressed in the incremental format [17-21]. The increment of viscoplastic volumetric strain rate can be approximated by

$$\ddot{\varepsilon}_p^{vp} \cong \frac{\dot{\varepsilon}_p^{vpt+\Delta t} - \dot{\varepsilon}_p^{vpt}}{\delta t} \tag{16}$$

in which δt is the time increment and $\dot{\varepsilon}_p^{vpt}$ and $\dot{\varepsilon}_p^{vpt+\Delta t}$ are the viscoplastic volumetric strain rates at the previous and current time steps, respectively. Substituting Eq. (16) into the consistency Eq. (12) yields

$$\mathbf{n}^T \dot{\boldsymbol{\sigma}}' m_p - \left(h + \frac{\xi_b}{\delta t}\right)\dot{\varepsilon}_p^{vpt+\Delta t} + \xi_b \ddot{\varepsilon}_p^{vpt} = 0 \tag{17}$$

Eq. (2) can be re-written as

$$\dot{\boldsymbol{\sigma}}' = \mathbf{D}^{\mathrm{e}}(\dot{\boldsymbol{\varepsilon}} - \dot{\boldsymbol{\varepsilon}}^{\mathrm{vp}}) = \mathbf{D}^{\mathrm{e}}\left(\dot{\boldsymbol{\varepsilon}} - \dot{\lambda}\mathbf{m}\right) \tag{18}$$

where $\dot{\lambda}$ is the viscoplastic multiplier. From Eq.s (17) and (18),

$$\dot{\lambda}^{t+\Delta t} = \frac{\mathbf{n}^T \mathbf{D}^{\mathrm{e}} \dot{\boldsymbol{\varepsilon}} + \xi_b^* \ddot{\varepsilon}_p^{vpt}}{\left(h + \frac{\xi_b}{\delta t} + \mathbf{n}^T \mathbf{D}^{\mathrm{e}} \mathbf{m}\right)} \tag{19}$$

where

$$\xi_b^* = \frac{\xi_b}{m_p} = -\frac{\partial F}{\partial \bar{p}_c'}\frac{\partial \bar{p}_c'}{\partial \varepsilon_p^{vp}}\frac{1}{\|\partial F/\partial \bar{\boldsymbol{\sigma}}'\|} \tag{20}$$

Substituting Eq. (19) into Eq. (18), the elasto-viscoplastic stress-strain relation is expressed as

$$\dot{\boldsymbol{\sigma}}' = \left(\mathbf{D}^e - \frac{\mathbf{D}^e\mathbf{m}\mathbf{n}^T\mathbf{D}^e}{h + \frac{\xi_b}{\delta t} + \mathbf{n}^T\mathbf{D}^e\mathbf{m}}\right)\dot{\boldsymbol{\varepsilon}} - \left(\frac{\mathbf{D}^e\mathbf{m}\xi_b^*\dot{\varepsilon}_p^{vp\,t}}{h + \frac{\xi_b}{\delta t} + \mathbf{n}^T\mathbf{D}^e\mathbf{m}}\right) \tag{21}$$

All the three stages of drained creep in geomaterials are captured by using the proposed bounding surface viscoplasticity model. In the case of single yield surface viscoplastic models, the creep process cannot be initiated from a stress state inside the yield surface and only begins when the stress point lies on the yield surface. Consequently, the hardening modulus h is always negative, and hence the first two phases of creep process cannot be captured. This is particularly important in the stability analysis of clayey slopes in which the creep-induced instability generally occurs at strengths less than the peak strength [22, 23].

3 Model Validation

3.1 Undrained Creep Tests on San Francisco Bay Mud

Stress-controlled laboratory tests on the creep behaviour under undrained conditions at different pressures and stress levels were carried out on San Francisco Bay Mud [24]. Three sets of tests were selected for the simulation, where the sustained deviator stress was maintained at 70%, 50% and 30% of the ultimate deviator stress (q_{ult}= 77.5 kPa) determined in the normal strength tests during undrained creep. The creep tests were continued for a two-week period, unless prior failure occurred.

The material parameters used in the simulations were: $\kappa = 0.01$ and $\lambda = 0.29$; $G = 14710$kPa, $M_{cs} = 1.44$, and $\Gamma = 4.3516$. The bounding surface material constants obtained from back-calculation of the test results as N and R define the shape of the bounding surface, A describes the stress–dilatancy relationship, and k_m calibrates the hardening modulus: $N = 1.02$, $R = 2.8043$, $A = 0.4$, and $k_m = 1.0$. The initial conditions of the samples were $p'_0 = 98.1$kPa and $e_0 = 2.3$. The viscoplastic parameter $c_\beta = 0.06$ was used in the simulations with the reference strain rate $\dot{\varepsilon}_{p,r}^{vp} = 10^{-3}$/min.

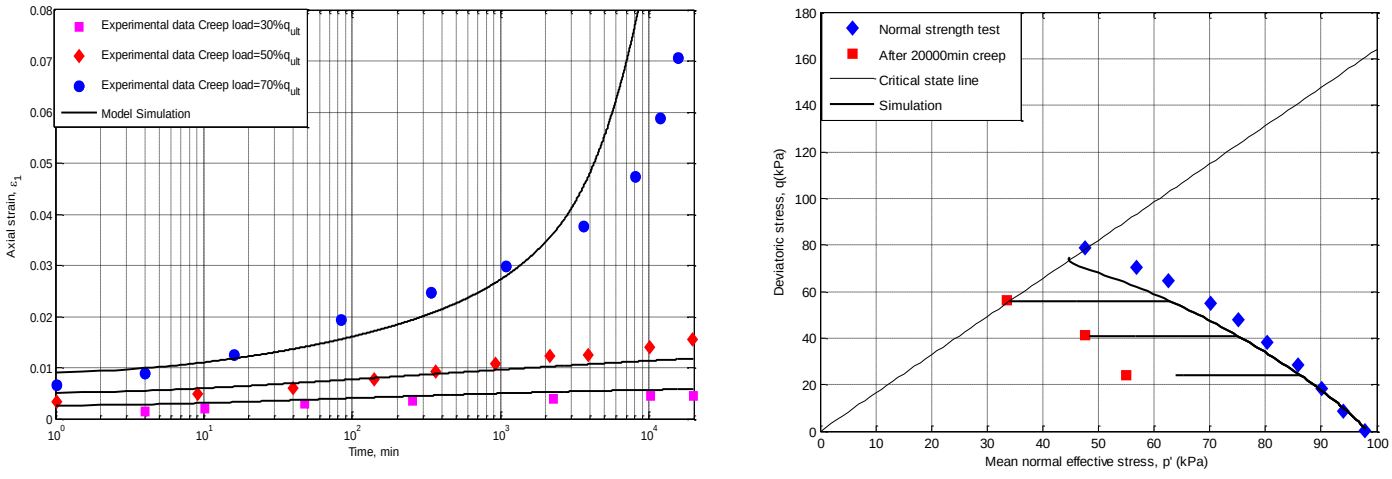

a) b)

Fig. 2. Simulation results and experimental data of undrained creep tests on San Francisco Bay Mud: a) Axial strain versus time; b) Deviatoric stress versus the mean normal effective stress

Figure. 2 presents the comparison between the measured data and the modelling results for the undrained creep tests on SFBM. As observed, the specimens subjected to creep loads of 30% and 50% of q_{ult} show only a small increase in axial strain,

while samples subjected to creep loads of 70% show large axial strain after the initial deformation, leading to creep rupture. As shown in Figure. 2, the model simulations match the experimental data well, demonstrating the capability of the proposed model in modelling the undrained creep behaviour of clayey soils.

3.2 Drained Creep Tests on Haney Clay

The drained triaxial creep tests were carried out on undisturbed heavily over-consolidated Haney Clay [25]. The sample was initially consolidated isotropically to effective stress of 517.1 kPa for 24 h and then rebounded to an effective stress of 20.7 kPa for 44 h. The initial conditions of the samples were $p'_0 = 20.7$ kPa and $e_0 = 0.667$. The sustained deviator stress level maintained during the drained creep test was 90% of the ultimate deviator stress.

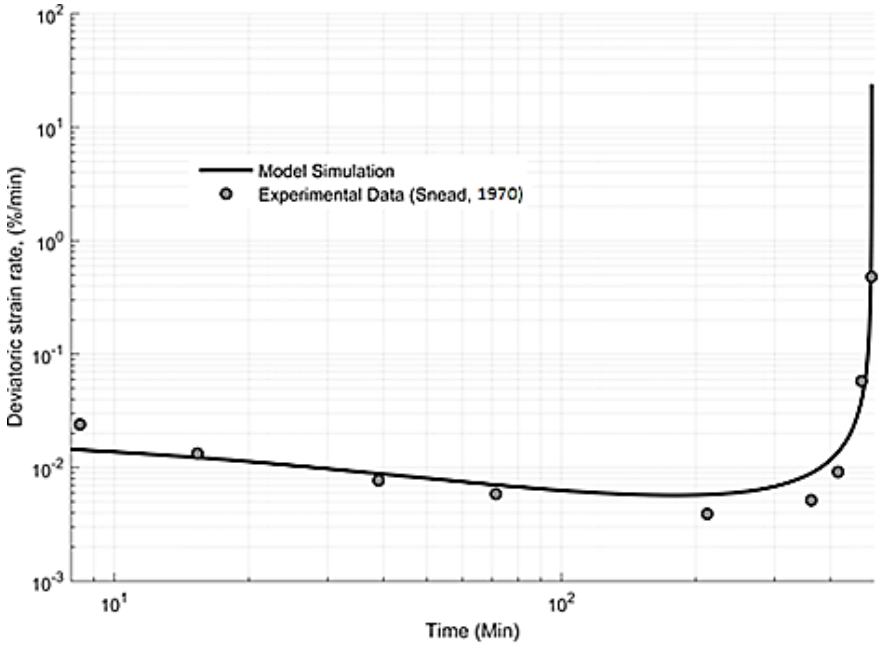

Fig. 3. Simulation results and experimental data of drained creep tests on Haney Clay: Deviatoric strain rate versus Time

The material parameters used in the simulations were calibrated using the experimental data. The model parameters were $\kappa = 0.018$ and $\lambda = 0.093$; $\nu = 0.3$, $M_{cs} = 1.39$, and $\Gamma_0 = 2.15$. The bounding surface material constants obtained from back-calculation of the test results as N and R define the shape of the bounding surface, A describes the stress–dilatancy relationship, and k_m calibrates the hardening modulus: $N = 2.5$, $R = 1.714$, $A = 1.72$ and $k_m = 9.7$. The viscoplastic parameter $c_\beta = 0.06$ was used in the simulations with the reference strain rate $\dot{\varepsilon}_{p,r}^{vp} = 10^{-6}$/min.

The simulation results of the drained creep test on Haney Clay are presented in Figure. 3 which depicts the variation of deviatoric strain rate with time. As observed, there is a good agreement between the experimental data and the modelling results. It is observed that the strain rate decreases over time during the primary phase of creep. In this phase, due to both increase in void ratio and decrease in viscoplastic volumetric strain rate, the compressive strength of the soil reduces. This leads the creep process into the secondary phase with a transient minimum strain rate of 0.004%/min. The further reduction of the compressive strength due to increase in void ratio leads the process into tertiary creep with increasing strain rate, leading to creep rupture.

4 Conclusions

A bounding surface viscoplasticity constitutive model is presented for the analysis of time-dependent behaviour of clay to capture tertiary creep and creep rupture. The model provides a continuous transition from rate-independent plasticity to rate-dependent viscoplasticity. The model is formulated within the critical state framework using the consistency theory. The elastic behaviour is captured through the isotropic elasticity rule, while the viscoplastic behaviour is captured through the hardening/softening effects of viscoplastic strain and viscoplastic strain rate on the size of the bounding surface. The hardening

parameter representing the size of the bounding surface is defined as a function of viscoplastic volumetric strain and viscoplastic volumetric strain rate. A non-associated flow rule is defined to generalize application of the model to a wide range of soils. The capability of the model to predict tertiary creep in drained and undrained conditions is also presented. The capability of the proposed model in describing creep process and creep failures in geomaterials is demonstrated through good agreements between the simulation results and the experimental data.

REFERENCES

[1]- P. Perzyna, On the constitutive equations for work-hardening and rate sensitive plastic materials. Bul. Acad. Pol. Sci. Serie des Sciences Techniques. 12(4) (1963) 199-206.

[2]- P. Perzyna, Fundamental problems in viscoplasticity. Adv. Appl. Mech. 9 (1966) 243-377. doi:doi.org/10.1016/S0065-2156(08)70009-7

[3]- T. Adachi, F. Oka, Constitutive equations for normally consolidated clay based on elasto-viscoplasticity. Soils. Found. 22(4) (1982) 57-70. doi:10.3208/sandf1972.22.4_57

[4]- V.N. Kaliakin, Y.F. Dafalias, Theoretical aspects of the elastoplastic-viscoplastic bounding surface model for cohesive soils. Soils. Found. 30(3) (1990) 11-24. doi:10.3208/sandf1972.30.3_11

[5]- B.L. Kutter, N. Sathialingam, Elastic - viscoplastic modelling of the rate-dependent behaviour of clays.Geotech. 42(3) (1992) 427-441. doi:10.1680/geot.1992.42.3.427

[6]- J.-H. Yin, J. Graham, Elastic viscoplastic modelling of the time-dependent stress-strain behaviour of soils. Can. Geotech. J. 36(4) (1999) 736-745. doi:10.1139/cgj-36-4-736

[7]- S. Kimoto, B. Shahbodagh Khan, M. Mirjalili, F. Oka, Cyclic elastoviscoplastic constitutive model for clay considering nonlinear kinematic hardening rules and structural degradation. Int. J. Geomech. 15(5) (2015) A4014005. doi:10.1061/(ASCE)GM.1943-5622.0000327

[8]- F. Oka, B. Shahbodagh, S. Kimoto, A computational model for dynamic strain localization in unsaturated elasto-viscoplastic soils. Int. J. Numer. Anal. Methods. Geomech. 43(1) (2019)138-165. doi:10.1002/nag.2857

[9]- B. Shahbodagh, H. Sadeghi, S. Kimoto, F. Oka, Large deformation and failure analysis of river embankments subjected to seismic loading. Acta Geotech. 15(6) (2020) 1381-1408. doi:10.1007/s11440-019-00861-3

[10]- H. Sekiguchi, Theory of undrained creep rupture of normally consolidated clay based on elasto-viscoplasticity. Soils. Found. 24(1) (1984) 129-147. doi:10.3208/sandf1972.24.129

[11]- T. Matsui, N. Abe, Verification of elasto-viscoplastic model of normally consolidated clays in undrained creep. In: Proceeding of the sixthInternational Conference onNumerical Methods in Geomechanics, 1988, pp. 453-459. doi:10.1201/9780203745366

[12]- Y. Qiao, A. Ferrari, L. Laloui, W. Ding, Nonstationary flow surface theory for modeling the viscoplastic behaviors of soils. Comput. Geotech.76 (2016). 105-119. doi:10.1016/j.compgeo.2016.02.015

[13]- N. Khalili, M.A. Habte, S. Zargarbashi, A fully coupled flow deformation model for cyclic analysis of unsaturated soils including hydraulic and mechanical hystereses. Comput. Geotech. 35(6) (2008) 872-889. doi:10.1016/j.compgeo.2008.08.003

[14]- W.M. Wang, L.J. Sluys, R. de Borst, Viscoplasticity for instabilities due to strain softening and strain-rate softening. Int. J. Numer. Meth. Eng. 40(20) (1997) 3839-3864. doi:10.1002/(sici)1097-0207(19971030)40:20<3839::aid-nme245>3.0.co;2-6

[15]- A. Carosio, K. Willam, G. Etse, On the consistency of viscoplastic formulations. Int. J. Solids. Struct. 37(48) (2000) 7349-7369. doi:10.1016/S0020-7683(00)00202-X

[16]- N. Khalili, M.A. Habte, S. Valliappan, A bounding surface plasticity model for cyclic loading of granular soils. I Int. J. Numer. Meth. Eng. 63(14) (2005) 1939-1960. doi:10.1002/nme.1351

[17]- T.N. Mac, B. Shahbodaghkhan, N. Khalili, A Constitutive Model for Time-Dependent Behavior of Clay. Int. J. Geo. Environ. Eng. 8(6) (2014) 596-601. doi:10.5281/zenodo.1092936

[18]- B. Shahbodagh, M. Mirjalili, S. Kimoto, F. Oka, Dynamic analysis of strain localization in water-saturated clay using a cyclic elasto-viscoplastic model.Int. J. Numer. Anal. Methods Geomech. 38(8) (2014) 771-793. doi:10.1002/nag.2221

[19]- T.N. Mac, B. Shahbodagh, N. Khalili, A Bounding Surface Viscoplastic Constitutive Model for Unsaturated Soils. In: Proceedings of the sixth Biot Conference on Poromechanics, Poromechanics 2017, Paris, 2017, pp. 1045-1052. doi:10.1061/9780784480779.130

[20]- B. Shahbodagh, M.A. Habte, A. Khoshghalb, N. Khalili, A bounding surface elasto-viscoplastic constitutive model

for non-isothermal cyclic analysis of asphaltic materials. Int. J. Numer. Anal. Methods Geomech. 41(5) (2017) 721-739. doi:10.1002/nag.2574

[21]- T.N. Mac, B. Shahbodagh, N. Khalili, A fully coupled flow-deformation model for time-dependent analysis of unsaturated soils. In: Proceedings of thesaventh Asia-Pacific Conference on Unsaturated Soils, Nagoya, 2019.

[22]- B. Shahbodagh, T.N. Mac, G.A. Esgandani, N. Khalili, A Bounding Surface Viscoplasticity Model for Time-Dependent Behavior of Soils Including Primary and Tertiary Creep. Int. J. Geomech. 20(9) (2020)04020143. doi:10.1061/(ASCE)GM.1943-5622.0001744

[23]- T.N. Mac, A Bounding Surface Viscoplasticity Model for Time dependent Behaviour of Saturated and Unsaturated Soils including Tertiary Creep, PhD Thesis, University of New South Wales, 2020.

[24]- K. Arulanandan, C.K. Shen, R.B. Young, Undrained creep behaviour of a coastal organic silty clay. Geotech. 21(4) (1971) 359-375. doi:10.1680/geot.1971.21.4.359

[25]- D.E. Snead, Creep rupture of saturated undisturbed clays, Ph,D Thesis, University of British Columbia, 1970.